Sulfate-Induced Effects in the On-Pathway Intermediate of the Bacterial Immunity Protein Im7* †

Eva S. Cobos and Sheena E. Radford*

Astbury Centre for Structural Molecular Biology, Garstang Building, University of Leeds, Leeds LS2 9JT, U.K.

Received October 18, 2005; Revised Manuscript Received December 21, 2005

ABSTRACT: Intermediates have now been identified in the folding of a number of small, single-domain proteins. Here we describe experiments to determine the effect of Na_2SO_4 on the properties of the on-pathway intermediate formed early during the folding of the four-helical protein, Im7*. This intermediate, studied previously in 0.4 M Na_2SO_4, contains three of the four native helices and is fascinating in that several residues in helices I, II, and IV make non-native interactions that stabilize this state. Whether these contacts form as a consequence of the presence of Na_2SO_4, however, remained unresolved. Using kinetic analysis of the effect of Na_2SO_4 on the unfolding and refolding kinetics of Im7*, combined with detailed analysis of the resulting chevron plots, we show that decreasing the concentration of Na_2SO_4 from 0.4 to 0 M destabilizes the intermediate and rate-limiting transition (TS2) states by 7 and 10 kJ mol^{-1}, respectively, and has little effect on the relative compactness of these states compared with that of the unfolded ensemble ($\beta_I \approx 0.8$, $\beta_{TS2} \approx 0.9$ in 0 to 0.4 M Na_2SO_4). Analysis of 10 variants of the protein in 0.2 M Na_2SO_4 using Φ-values showed that the structural properties of the intermediate and TS2 are not altered significantly by the concentration of the kosmotrope. The data demonstrate that the rapid formation of a compact intermediate stabilized by non-native interactions during Im7* folding is not induced by high concentrations of the stabilizing salt, but is a generic feature of the folding of this protein.

While intermediates are commonly formed during the folding of many large (>100 residue) proteins and many have been characterized in detail (*1*, *2*), partially folded states have only recently been identified during the folding of small, single-domain proteins as techniques capable of their detection using rapid measurements have been developed. In many cases, detection of intermediates during the folding of small proteins has required alteration of the solution conditions and/or changes in the sequence of the polypeptide such that intermediates become visibly populated (*3*−*11*). One of the most common routes used to detect compact states early during folding is by the addition of stabilizing salts (kosmotropes), which can affect protein structure through direct interaction with the protein or through effects on water structure, depending on the salt concentration used (*6*, *12*, *13*). Thus, at low salt concentrations electrostatic interactions can increase protein stability, while high concentrations of kosmotropes stabilize proteins through their effect on water structure and preferential exclusion of the ions from the protein surface (*14*). Sodium sulfate is one of the most commonly used salts for this purpose (*15*), and the addition of high concentrations of Na_2SO_4[1] (usually at least 0.4 M) has been shown to stabilize burst-phase intermediates in several proteins (*6*, *12*, *13*, *16*−*19*). While some argue that Na_2SO_4 stabilizes species already present on the reaction coordinate, but which are too unstable or too transient to detect in the absence of salt (*16*, *20*), others have suggested that the generic stabilization of compact states by Na_2SO_4 results in the formation of misfolded or off-pathway species, which otherwise would not be encountered during productive folding (*12*).

Here we describe the effect of Na_2SO_4 on the folding mechanism of Im7, a four-helical protein belonging to the bacterial immunity protein family, which share ∼60% sequence homology (*21*). The folding landscape of these closely homologous proteins is finely balanced, such that small changes in sequence or minor alterations in the folding conditions can switch the kinetic mechanism of folding from two- to three-state (*5*, *22*−*24*). For example, Im7-folding involves the population of an on-pathway intermediate which is stabilized at pH 7.0 by the presence of 0.4 M Na_2SO_4 (*13*, *25*, *26*). The intermediate has been analyzed using stopped flow and ultra-rapid mixing fluorescence in combination with hydrogen exchange methods (*25*−*27*) and has been shown to be compact ($\beta_I = 0.8$) and hyperfluorescent (the intermediate is more fluorescent than both the native and denatured states) (*13*). The intermediate also contains three of the four native helices, while the short (6-residue) helix III is formed only after the rate-limiting transition state has been traversed (*26*) (Figure 1). Importantly, in the absence of helix III, helices I, II, and IV that form early

† E.S.C. was supported by the awards of a FEBS Fellowship and by the Institute for Molecular Biophysics, University of Leeds. S.E.R. is a BBSRC Professorial Fellow.

* To whom correspondence should be addressed: Telephone: 0113 343 3170. Fax: 0113 343 3167. E-mail: s.e.radford@leeds.ac.uk.

[1] Abbreviations: Im7*, hexa-histidine-tagged Im7; Na_2SO_4, sodium sulfate; wt, wild-type; K_{X-Y}, the equilibrium constant between *X* and *Y*; k_{xy}, the rate constant of folding/unfolding from *x* to *y*; M_{X-Y}, the urea-dependence of $-RT \ln K_{xy}$; m_{xy}, the urea dependence of $-RT \ln k_{xy}$; $\Delta\Delta G_{X-Y}$, the change in the difference in the Gibbs energy between *X* and *Y*.

10.1021/bi0521238 CCC: $33.50
Published on Web 01/31/2006

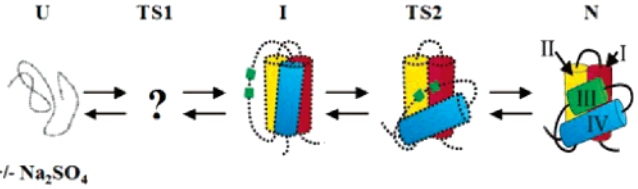

FIGURE 1: Reaction scheme of the folding mechanism of Im7* at pH 7.0 and 10 °C. The native helices I, II, and IV are colored red, yellow, and blue. Residues in helix III are shown in green. U, unfolded state; I, intermediate state; N, native state; TS1 and TS2, early and rate-determining transition states, respectively. While the structural characteristics of the intermediate ensemble and TS2 have been determined using equilibrium methods and Φ-value analysis (*26*, *55*), precisely how helices I, II, and IV dock in I and TS2 is not currently known and their orientations shown here is arbitrary. There is currently no knowledge about the conformational properties of U and TS1.

during folding dock in a non-native manner, such that the partially folded species is stabilized by both native and non-native interactions involving side chains in these helices, including the single tryptophan (Trp 75) (*26*, *28*). To form the native state, helices I, II, and IV must then reorganize, allowing helix III to dock onto the structure, effectively trapping the protein in the native conformation.

The importance of non-native interactions in stabilizing the intermediate state in Im7-folding provides an opportunity to tailor the ruggedness of the landscape with unprecedented precision. For example, decreasing the pH from 8.0 to 6.0 stabilizes the folding intermediate but has little effect on the stability of native Im7* (a hexa-histidine tagged version of the protein), such that the ruggedness of the landscape is increased (*5*). By contrast with Im7, the homologue Im9 folds with two-state kinetics at pH 7.0 (*5*, *13*). However, the folding mechanism of Im9 can be switched to three-state kinetics by introducing substitutions at solvent exposed positions which increase the helical propensity of helices I, II, or IV (*24*). Alternatively, stabilizing non-native interactions by amino acid substitutions at specific sites designed on the basis of the properties of the Im7 folding intermediate (*23*) or reducing the pH (*5*) also results in Im9 folding to the native conformation via a populated three-helical intermediate. Together with information from UV resonance Raman spectroscopy that indicates that Trp75 experiences a more hydrophobic environment in the partially folded intermediate of Im7* than in the native protein (*28*), these data suggest that specific non-native interactions involving aromatic and aliphatic side chains play a critical role in the folding of this protein.

Despite the detailed information obtained to date about the folding mechanism of Im7*, the role of Na_2SO_4 in this process and, specifically, whether folding via a three-helical intermediate stabilized by both native and non-native interactions results as a consequence of the addition of 0.4 M Na_2SO_4, remained unresolved. To address these issues, we have reinvestigated the folding mechanism of Im7* as a function of the concentration of Na_2SO_4 (0−0.4 M) using stopped-flow fluorescence and have analyzed the results in detail, taking account of possible movements in the ground states, and transient population of the intermediate during both folding and unfolding as a function of the concentration of the kosmotrope. Ten variants selected from those used previously to determine the folding mechanism of Im7* in 0.4 M Na_2SO_4 (*26*) are also reanalyzed in 0.2 M Na_2SO_4 (the lowest concentration of Na_2SO_4 in which the intermediate is sufficiently stable to permit Φ-value analysis) to provide structural details about the intermediate and rate-limiting transition states for folding at the lower concentration of the stabilizing salt.

MATERIALS AND METHODS

Im7 Purification*. Im7* and the variants used for Φ-value analysis were overexpressed and purified as described (*5*).

Data Collection and Analysis. All measurements were performed at 10 °C using an Applied Photophysics SX18.MV stopped-flow fluorimeter, and normalized as described previously (*5*, *29*).

The urea-dependence of the rate constants of folding and unfolding of Im7* and its variants were fitted to a three state on-pathway model using the nonlinear least-squares fitting method in OriginPro 7.5 (Hearne Scientific Software):

Scheme 1

$$U \underset{k_{iu}}{\overset{k_{ui}}{\rightleftharpoons}} I \underset{k_{ni}}{\overset{k_{in}}{\rightleftharpoons}} N$$

where U, I, and N are the unfolded, intermediate, and native states, respectively and used to obtain the values K_{U-I} ($= k_{ui}/k_{iu}$), k_{in} and k_{ni} and the corresponding m-values M_{U-I} ($= m_{ui} - m_{iu}$), m_{in}, and m_{ni}. Since only the equilibrium properties of the intermediate K_{U-I} and M_{U-I} are described by the stopped flow data, k_{ui} was fixed to 3000 s^{-1}, using the value for this constant previously measured for the wild-type protein using ultra-rapid mixing (*25*). Only for variants displaying an unfolding roll-over was k_{ui} allowed to vary from this value to obtain an adequate fit to these data.

To obtain accurate values for the rate constants and their respective m-values both the urea-dependence of the rate constants and the associated kinetic amplitudes (the initial and final fluorescence signals) were used to fit the data. Initially, only the urea-dependence of rate constants was fitted. Once an adequate fit to the rate constants was obtained the urea dependence of the initial and final fluorescence signals was also considered. Only parameters that resulted in a good fit to both sets of data, which was judged from the chi-squared statistic as well as an accurate reproduction of the fluorescence signals versus the concentration of urea, were considered as an adequate fit to the data. Note that while the rate constant can be accurately measured with high reproducibility (within ±5%), analysis of the fluorescence signals is subject to a larger error (±10%). This was taken into consideration when judging the goodness of fit of the data.

The chevron plot for each variant and for the wild-type protein at a concentration of 0.2−0.4 M Na_2SO_4 was fitted individually. The data for the wild-type protein as a function of the concentration of Na_2SO_4 was also fitted globally, sharing values for m_{ui} (2.6 ± 0.5 kJ mol^{-1} M^{-1}) and m_{in} (0.6 ± 0.1 kJ mol^{-1} M^{-1}) which were shown using the individual fits not to vary significantly versus the concentration of Na_2SO_4. No significant differences were observed when the results from the individual fits and the fits sharing parameters were compared. Global analysis thus allowed accurate fitting of all curves, irrespective of the stability of I.

In all fits, the fluorescence signals of U, I, and N in H_2O and the urea-dependences of these signals were assumed not to vary for the different variants and different solution conditions studied. For wild-type Im7* in 0, 0.1, and 0.4 M Na_2SO_4 and most variants values the fluorescence signals of U, I, and N were 0.675 + 0.04 [urea], 1.15 + 0.02 [urea], and 0.265 + 0.02 [urea], respectively. For wild-type Im7* in 0.2 and 0.3 M Na_2SO_4 the fluorescence signal of I was altered to 1.35 + 0.02 [urea] and 1.27 + 0.02 [urea], respectively, to adequately describe the initial signal. Similarly for the variants L3A, L34A, V42A, and I44V in 0.2 M Na_2SO_4, the fluorescence signal of I was altered to 0.75 + 0.02 [urea], 0.59 + 0.02 [urea] 0.95 + 0.02 [urea], and 1.25 ± 0.02 [urea], respectively.

Fitting Data to Chevron Plots Showing Significant Curvature in the Unfolding Branch. The variants I22V, L34A, and L38A displayed significant curvature in the unfolding branch. The folding and unfolding kinetics of these variants was also fitted to the three-state on-pathway model, assuming that the same intermediate is transiently populated during both folding and unfolding. Alternative models, including a model involving a switch or movement in the rate-limiting transition state (*30*) were not able to fit the data satisfactorily. For I22V k_{ui} was fixed to 1000 s^{-1} to obtain a satisfactory fit to the data, while for L34A it was necessary to vary k_{ui}, keeping a fixed k_{iu} of 50 s^{-1}. Both parameters were altered to obtain a satisfactory fit to the data for L38A. Data obtained previously for L34A and L38A in 0.4 M Na_2SO_4 (*26*) which also show a significant deviation from linearity in the unfolding branch of the chevron plot were refitted in this manner.

Calculation of the Stability of N and I States and β-Tanford Values. The stability of N and I were estimated from the fit to eq 1 according to:

$$\Delta G_{U-N} = -RT \ln\left(\frac{k_{in}}{k_{ni}} \cdot \frac{k_{ui}}{k_{iu}}\right) \quad (1)$$

$$\Delta G_{U-I} = -RT \ln\left(\frac{k_{ui}}{k_{iu}}\right) \quad (2)$$

where the ratio k_{ui}/k_{iu} represents the value of the equilibrium constant between U and I (K_{U-I}).

The respective *m*-values were also calculated from the fit of the data using:

$$M_{U-I} = m_{ui} - m_{iu} \quad (3)$$

$$M_{U-N} = m_{ui} - m_{iu} + m_{in} - m_{ni} \quad (4)$$

The position of the intermediate (β_I) and rate-limiting transition state (β_{TS2}) along the reaction coordinate are defined from the kinetic *m*-values by:

$$\beta_I = \frac{M_{U-I}}{M_{U-N}} \quad (5)$$

$$\beta_{TS2} = \frac{M_{U-I} + m_{in}}{M_{U-N}} \quad (6)$$

Φ-Value Analysis. Φ_I and Φ_{TS2}-values are defined in eqs 7 and 8:

$$\Phi_I = \frac{\Delta G^m_{U-I} - \Delta G^{wt}_{U-I}}{\Delta G^m_{U-N} - \Delta G^{wt}_{U-N}} \quad (7)$$

$$\Phi_{TS2} = \frac{\left((\Delta G^m_{U-I} - \Delta G^{wt}_{U-I}) - \left(RT \ln\left(\frac{k^m_{in}}{k^{wt}_{in}}\right)\right)\right)}{(\Delta G^m_{U-N} - \Delta G^{wt}_{U-N})} \quad (8)$$

where the superscripts m and wt refer to the mutant and wild-type species, respectively. Substitution of eqs 1 and 2 into 7 and 8 were used to obtain the expressions used to calculate the Φ_I- and Φ_{TS2}-values determined from the microscopic rate constants for folding and unfolding:

$$\Phi_I = \frac{\ln\left(\frac{k^m_{ui}}{k^m_{iu}} \Big/ \frac{k^{wt}_{ui}}{k^{wt}_{iu}}\right)}{\ln\left[\frac{\left(\left(\left(\frac{k^m_{ui}}{k^m_{iu}}\right)k^m_{in}\right)\Big/k^m_{ni}\right)}{\left(\left(\left(\frac{k^{wt}_{ui}}{k^{wt}_{iu}}\right)k^{wt}_{in}\right)\Big/k^{wt}_{ni}\right)}\right]} \quad (9)$$

$$\Phi_{TS2} = \frac{\ln\left(\left(\left(\frac{k^m_{ui}}{k^m_{iu}}\right)k^m_{in}\right) \Big/ \left(\left(\frac{k^{wt}_{ui}}{k^{wt}_{iu}}\right)k^{wt}_{in}\right)\right)}{\ln\left[\frac{\left(\left(\left(\frac{k^m_{ui}}{k^m_{iu}}\right)k^m_{in}\right)\Big/k^m_{ni}\right)}{\left(\left(\left(\frac{k^{wt}_{ui}}{k^{wt}_{iu}}\right)k^{wt}_{in}\right)\Big/k^{wt}_{ni}\right)}\right]} \quad (10)$$

Estimation of Errors. Errors for K_{U-I}, ΔG_{U-N}, ΔG_{U-I}, M_{U-N}, M_{U-I}, β_I, β_{TS2} were propagated from errors in the individual parameters k_{iu}, k_{in}, k_{ni}, m_{ui}, m_{iu}, m_{in} and m_{ni}. Errors in Φ_I and Φ_{TS2} were calculated from the partial derivatives of eqs 9 and 10 using MAPLE 9.5 (Adept Scientific).

RESULTS

Folding and Unfolding Kinetics of Im7 as a Function of the Concentration of Na_2SO_4*. The folding and unfolding kinetics of Im7*, measured using stopped-flow fluorescence in the presence of 0−0.4 M Na_2SO_4 at 10 °C, are shown in Figure 2. Previous results using higher concentrations of this salt (0.4 up to 1 M) have shown that the compactness of the intermediate does not increase above 0.4 M Na_2SO_4 at the pH and temperature used in the present study (*5*). Thus, higher concentrations of Na_2SO_4 were not considered here. The data show that, as the concentration of Na_2SO_4 is decreased from 0.4 to 0 M, the unfolding rate constants are increased (Figure 2A), and the native state is destabilized as indicated by the shift in the midpoint of the final fluorescence signal toward lower concentrations of urea (Figure 2B). In addition, the nonlinearity observed in the logarithm of the folding rate constant versus the concentration of urea (the "roll-over") becomes much less apparent as the concentration

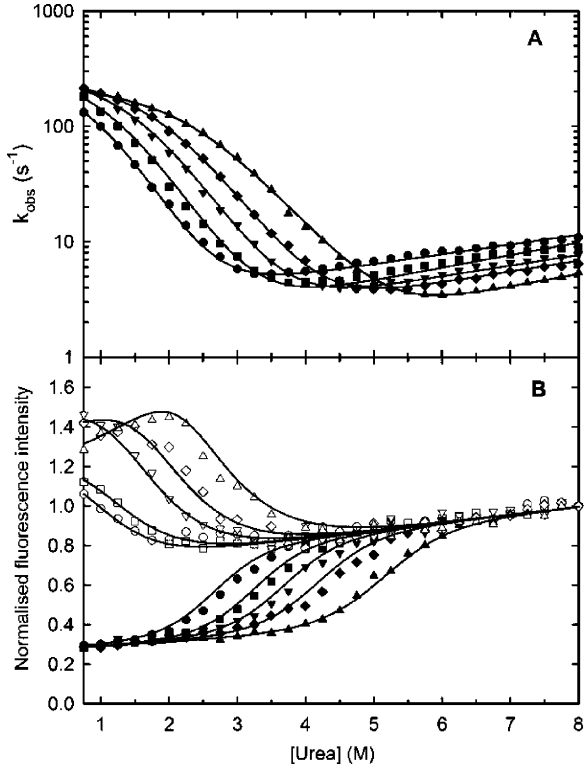

FIGURE 2: Folding and unfolding kinetics of Im7* at different concentrations of Na_2SO_4. (A) The urea-dependence of unfolding and folding rate-constants obtained by stopped-flow fluorescence. The concentration of Na_2SO_4 is 0.0 M (circles), 0.1 M (squares), 0.2 M (down triangles), 0.3 M (diamonds), and 0.4 M (up triangles). All data were obtained at pH 7.0 at 10 °C. Continuous lines show the best fit to the three-state on-pathway model (see Methods). (B) The urea-dependence of the initial (open symbols) and final (filled symbols) fluorescence signals obtained from the refolding kinetics. Solid lines represent the best fit to the three-state on-pathway model (see Methods).

of Na_2SO_4 is decreased, consistent with significant destabilization of the intermediate as the concentration of Na_2SO_4 is decreased. Importantly, the roll-over remains a clear feature of the chevron plot in 0 M Na_2SO_4, consistent with retention of a three-state folding mechanism even in the absence of the kosmotrope (Figure 2A and (*13*)). In accord with this, analysis of the effect of Na_2SO_4 on the urea dependence of the initial fluorescence signal also shows that the burst-phase intermediate (which is more fluorescent than both the native and denatured states) remains significantly populated even in the absence of the stabilizing salt (Figure 2B).

The data shown in Figure 2 were fitted both individually and globally to a three-state on-pathway model (see Methods), and the resulting thermodynamic parameters are shown in Table 1. The data show that the microscopic folding rate constant in water, k_{in}, does not change significantly versus the concentration of Na_2SO_4, indicating that the stabilities of the intermediate and rate-limiting transition states (TS2) respond similarly to the concentration of Na_2SO_4. By contrast, decreasing the concentration of Na_2SO_4 results in a decrease in ΔG_{U-N} and ΔG_{U-I}, indicating that both the intermediate and native states are destabilized as the concentration of Na_2SO_4 is lowered ($\Delta\Delta G_{U-N} = -9.6$ kJ mol^{-1} and $\Delta\Delta G_{U-I} = -7.6$ kJ mol^{-1} (0.4 to 0 M Na_2SO_4)) (Table 1). Consistent with previous results (*13*), therefore, the data indicate that Im7 folds via a three-state mechanism involving the population of an intermediate in the first 3 ms of folding even in the absence of Na_2SO_4.

The Effect of Na_2SO_4 on the Position of the Intermediate and TS2 on the Reaction Coordinate. It is well-known for many reactions in organic chemistry that there is a linear relationship between the change in the rate of a chemical reaction with the change in stability of the ground states, caused, for example, by changes in pH, temperature, or salt concentration (*31*). These rate-equilibrium free energy relationships, REFERs, have also been used in protein folding studies to characterize the properties of the transition state relative to the ground states when perturbations are applied to the system (*32*). For example, in situations where the relative compactness of the ground states of a reaction are known to be invariant to changes in the solution conditions, changes in the apparent compactness (the β_T value) of the transition state as the stability of the native state is decreased have been interpreted as a movement of the transition state toward the native conformation—the so-called Hammond effect (*33*, *34*). For many proteins β_I and β_{TS} values have been shown to remain constant over a broad range of $\Delta\Delta G_{U-N}$ values, indicating little effect of a free energy perturbation on the structure of the intermediate and rate-limiting transition states (*35*). In other cases, however, significant changes in β_I and β_{TS} values as $\Delta\Delta G_{U-N}$ varies suggest structural changes in the intermediate and rate-limiting transition states as protein stability changes (*35*). Thus, the characterization of REFERs can provide important information about the position of the transition state (following Hammond behavior) or changes in the ground states of a reaction upon perturbation.

To determine whether the inclusion of Na_2SO_4 increases the apparent compactness of the intermediate and rate-limiting transition states of Im7* folding, a detailed analysis of the equilibrium and kinetic *m*-values obtained in 0−0.4 M Na_2SO_4 was undertaken (Table 1). Different possible scenarios for the effect of Na_2SO_4 on the folding reaction coordinate for a three-state reaction involving an on-pathway intermediate are depicted in Figure 3. Although Hammond behavior and ground-state effects are both related to changes in observed β_T values, these effects can be distinguished by careful comparison of the effect of the perturbation on the equilibrium and kinetic *m*-values (distinguished here by the use of upper case M_{X-Y} value for equilibrium parameters, while the lower case m_{xy} value is used to denote the kinetic parameter). Thus, when the native state is destabilized (e.g. by decreasing the Na_2SO_4 concentration) and the rate-limiting transition state demonstrates Hammond behavior (case 2, Figure 3), no change in M_{U-N} is observed, while m_{u-TS2} increases. By contrast, when a ground-state effect occurs and the position of the transition state is not altered, M_{U-N} is decreased (or increased) due to changes in the structure of the unfolded or native states (Figure 3, cases 3 and 4, respectively). Thus, constant M_{X-Y} values indicate the absence of changes on the ground states, while changes in this parameter suggest changes to at least one of the ground states by the perturbation applied. Finally, by comparison of the kinetic and equilibrium *m*/*M*-values whether ground-state effects result from changes in the unfolded or native states can be discerned. Using such an approach, Sanchez and Kiefhaber have analyzed 21 different proteins and have shown (with the notable exception of CI2 (*32*)) that apparent

Table 1: Kinetic Parameters from the Global Fit of the Folding/Unfolding Kinetics of Im7* at 10 °C and Different Concentrations of Na_2SO_4[a]

$[Na_2SO_4]$	K_{U-I}	k_{in}	k_{ni}	m_{in}	m_{ni}	M_{U-I}	M_{U-N}	ΔG_{U-I}	ΔG_{U-N}	β_I	β_{TS2}
0.0	10 ± 4.6	246 ± 29.8	2.4 ± 0.7	0.6 ± 0.1	−0.46 ± 0.11	5.12 ± 0.86	6.18 ± 0.87	−5.4 ± 1.1	−16.3 ± 1.3	0.83 ± 0.18	0.93 ± 0.14
0.1	15 ± 4.9	282.4 ± 16.4	1.3 ± 0.6	0.6 ± 0.1	−0.59 ± 0.15	4.70 ± 0.76	5.89 ± 0.79	−6.4 ± 0.8	−19.0 ± 1.3	0.80 ± 0.17	0.90 ± 0.13
0.2	35.3 ± 11.9	281.8 ± 8.3	1.4 ± 0.8	0.6 ± 0.1	−0.50 ± 0.19	4.60 ± 0.72	5.70 ± 0.76	−8.4 ± 0.8	−20.9 ± 1.5	0.81 ± 0.17	0.91 ± 0.13
0.3	75.0 ± 32.7	273 ± 7.1	1.2 ± 0.9	0.6 ± 0.1	−0.50 ± 0.25	4.39 ± 0.72	5.49 ± 0.77	−10.2 ± 1.1	−22.8 ± 1.9	0.79 ± 0.17	0.91 ± 0.13
0.4	200.0 ± 129.7	252.3 ± 8.5	0.8 ± 1.1	0.6 ± 0.1	−0.55 ± 0.48	3.90 ± 0.90	5.05 ± 1.02	−12.5 ± 1.5	−25.9 ± 3.6	0.77 ± 0.24	0.89 ± 0.18

[a] All data were fitted to the on-pathway three state model (see Methods). Units: $[Na_2SO_4]$ (M); k_{xy} (s^{-1}); m_{xy} (kJ mol^{-1} M^{-1}); ΔG_{X-Y} (kJ mol^{-1}). Errors shown correspond to the fitting errors and the propagated errors thereof.

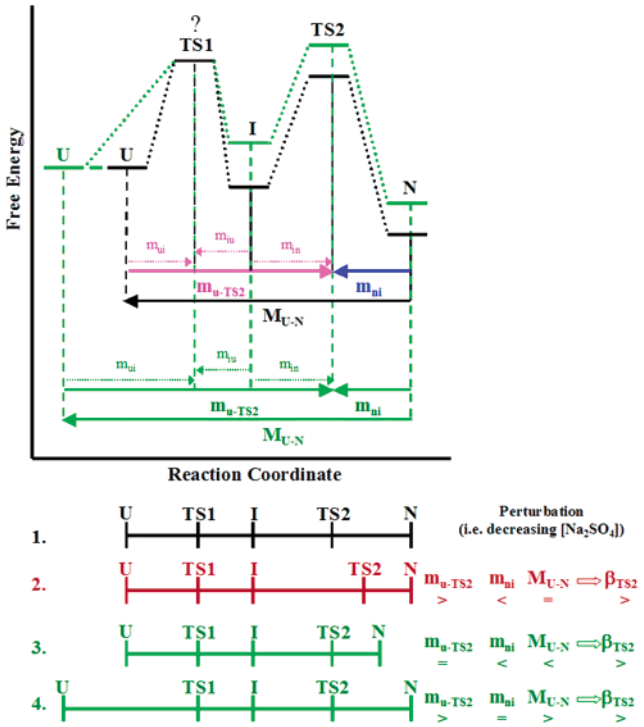

FIGURE 3: Illustration of possible effects induced by a perturbation on the position of ground states and the rate-limiting transition state (TS2) for the three-state on-pathway model. For simplicity, TS1 is not considered since this species cannot be characterized using stopped-flow methods. For clarity, the possible effects of a perturbation on the intermediate state are not depicted here, but these effects can be analyzed in a manner similar to those depicted for TS2 in cases 2−4. The scheme is an extension of that shown by Sanchez and Kiefhaber (*56*). 1 - reference situation. 2 - movement of TS2 following Hammond behavior. 3 - apparent movement of TS2 due to a ground-state effect on the native state. 4 - apparent movement of TS2 due to a ground-state effect on the unfolded state.

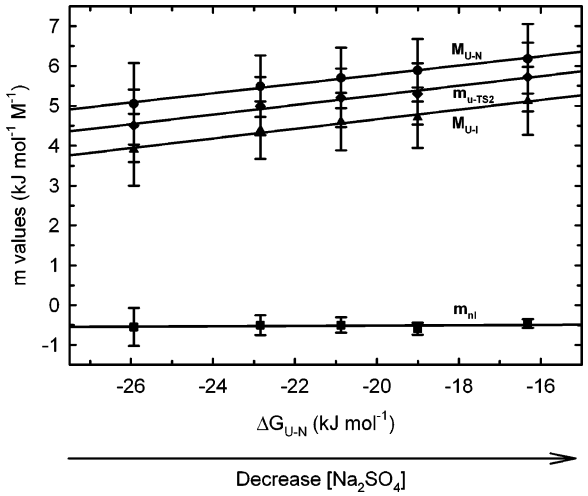

FIGURE 4: Dependence of M_{U-N} (circles), M_{U-I} (triangles), m_{u-TS2} (diamonds), and m_{ni} (squares) on ΔG_{U-N}, determined by altering the concentration of Na_2SO_4. The solid lines represent the weighted linear fit of the data.

movements in the transition states of many protein folding reactions upon mutation can be described by ground-state effects, rather than Hammond behavior (*35*).

The dependence of M_{U-N}, M_{U-I}, m_{u-TS2} and m_{ni} on ΔG_{U-N} for the folding transition of Im7* in different concentrations of Na_2SO_4 is shown in Figure 4. The data show that as the stability of native Im7* is decreased M_{U-N}, M_{U-I}, m_{u-TS2} increase slightly while m_{ni} remains constant. While such data would be consistent with a decrease in the compaction of the denatured state as the concentration of the kosmotrope decreases, none of these parameters changes significantly relative to the experimental error of fitting these parameters (Table 1). These data indicate, therefore, that the addition of Na_2SO_4 does not lead to a significant increase in compactness of the intermediate during Im7* folding. Instead, this species remains similarly compact even when it is only marginally populated. The data also indicate that the addition of Na_2SO_4 has no significant effect on the compaction of the unfolded state and rate-limiting transition state. Whether more subtle changes in the relative compactness of these states occurs during folding, as perhaps suggested by the systematic increase in M_{U-N}, M_{U-I} and m_{u-TS2} values as ΔG_{U-N} decreases (Figure 4), cannot be resolved beyond the errors associated with fitting the data.

Does the On-Pathway Intermediate Misfold at Low Concentrations of Na_2SO_4? While the above analysis indicates that the compactness of the intermediate and rate-limiting transition states of Im7* do not depend on the concentration of Na_2SO_4, the question remained whether the addition of the kosmotrope causes changes in the conformational properties of these species. In particular, whether the intermediate of Im7* retains the same three-helical structure stabilized by the unusual and striking mispacking of side chains observed previously in 0.4 M Na_2SO_4 (*26*) remained an open question. Importantly, of the 27 residues altered in the previous Φ-value analysis of Im7* folding in 0.4 M Na_2SO_4, 16 variants result in values of $\Delta\Delta G_{U-N}$ high enough for accurate Φ-value analysis (*36*), and of these, seven result in values of Φ_I that exceed Φ_{TS2} by 0.1−0.9 (*26*), confirming the validity of the interpretation that nonnative interactions are an important and characteristic feature of Im7* folding. To determine the conformational properties of the intermediate at lower concentrations of Na_2SO_4 the folding and unfolding kinetics of 10 of the variants studied previously in 0.4 M Na_2SO_4 (*26*) were reanalyzed in 0.2 M Na_2SO_4 (the lowest concentration of Na_2SO_4 in which the intermediate is sufficiently stable to permit Φ-value analysis). Residues were chosen that span the four helices of the native protein (L3A (N-terminal region), V16A and I22V (Helix

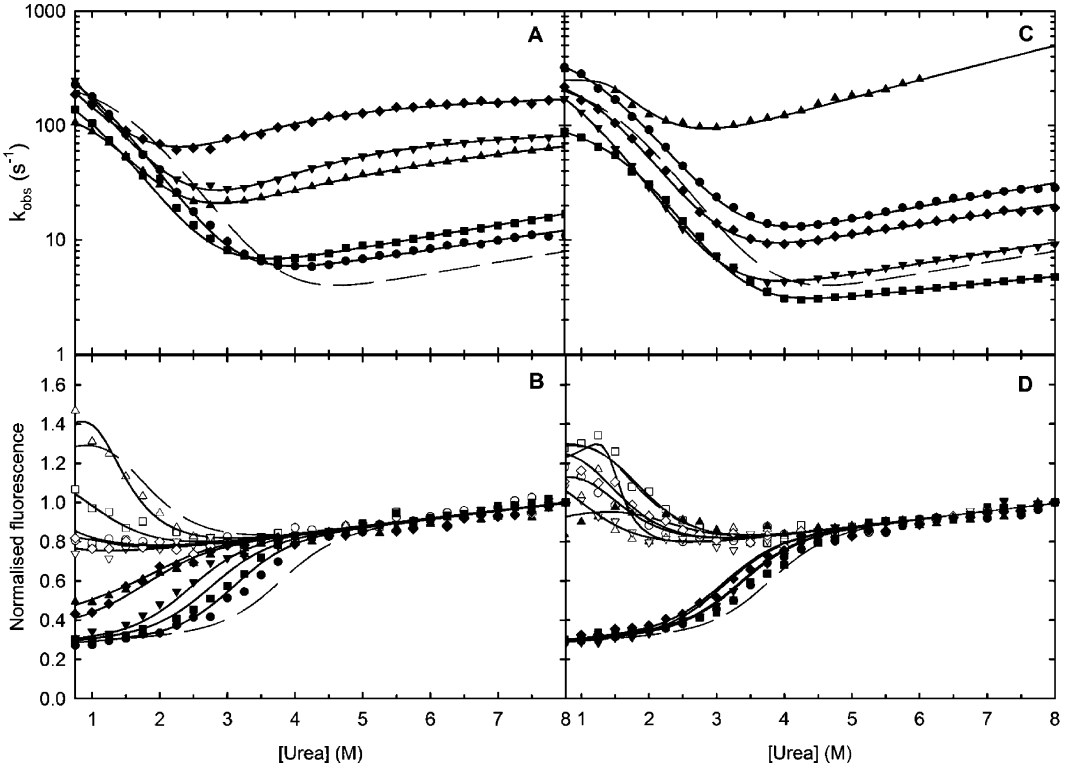

FIGURE 5: Folding and unfolding kinetics of wild-type Im7* and 10 variants at 10 °C and 0.2 M Na_2SO_4. (A,C) The urea-dependence of the unfolding and folding rate constants obtained by stopped-flow fluorescence for (A) L3A (circles); V16A (squares); I22V (up triangles); L34A (down triangles) and L38A (diamonds) and (C) V42A (circles); I44V (squares); L53A (up triangles); I68V (down triangles) and V69A (diamonds). The continuous lines show the best fit to on-pathway three-state model (see Methods). The data for wild-type Im7* are shown as a gray dashed line. (B,D) The urea-dependence of the initial (open symbols) and final (filled symbols) fluorescence signals from the refolding kinetics of these variants. Solid lines represent the best fit to the three-state model. The fluorescence signals obtained for wild-type Im7* are included for comparison (gray dashed lines).

I), L34A, L38A, V42A, and I44V (Helix II), L53A (Helix III), and I68V and V69A (Helix IV)), including several (L3A, L34A, L38A, V42A, and I68V) that report on the formation of non-native interactions. In all cases, the rate constants for folding and unfolding, as well as the initial and final fluorescence signals, were measured so as to provide the most accurate measurements of all kinetic parameters possible.

Chevron plots and the associated initial and final fluorescence signals for the 10 variants of Im7* studied in 0.2 M Na_2SO_4 are shown in Figure 5A−D. All variants were destabilized significantly relative to wild-type Im7*, as demonstrated either by an increase in the rate constant for unfolding and/or a decrease in the rate constant for folding. Consistent with this, a decrease in the midpoint of denaturation of the native protein is observed, judged from the urea dependence of the final fluorescence signals (Figure 5B,D). Interestingly, three of the variants studied (I22V, L34A, and L38A) show clear nonlinearity in the unfolding branch of their chevron plots (Figure 5A,C). Such a feature can arise from several scenarios, including the presence of unfolding intermediates (*37*), broad energy barriers in the reaction coordinate permitting movements in the rate-limiting transition state (*34*, *38*), or a switch in the rate-limiting step (*4*, *22*, *30*, *39*, *40*). Previous data on Im7* unfolding in 0.4 M Na_2SO_4 for F15A, L34A, L37A, L38A, and F41L also showed this feature, while it was not observed for I22V (*26*). Since the denaturant dependence of the initial signal shows that the intermediate in Im7* folding remains populated in 0.2 M Na_2SO_4 for 8 of the 10 variants (Figure 5B,D) the data were fitted to the on-pathway model, assuming that the same intermediate becomes transiently populated during both folding and unfolding (see Methods). As shown in Figure 5, an excellent fit to the data was obtained for all variants without the need to invoke more complex models. The resulting kinetic and thermodynamic parameters are shown in Table 2. Consistent with our previous analysis of Im7* folding using ultra-rapid mixing (*25*), the data provide further evidence that the intermediate in Im7* folding is on-pathway, since this species is populated during both folding and unfolding.

Φ_I and Φ_{TS2}-values for the 10 variants of Im7* in 0.2 M Na_2SO_4, determined as described in the Methods section, are summarized in Figure 6, and the resulting parameters are listed in Table 2. As occurs in 0.4 M Na_2SO_4, residues with high Φ_I-values (>0.3) are obtained for residues V16A, L38A, and I68V in helices I, II, and IV, while the Φ_I-value for L53A in helix III is close to zero, consistent with Im7* folding via a three-helical intermediate at the lower concentration of Na_2SO_4 studied here. For six residues (V16A, I22V, I44V, L53A, I68V, and V69A), the Φ_I-values remain unchanged or increase in TS2, consistent with the structure in the intermediate becoming consolidated as the transition state is reached. Interestingly, however, for L3A, L34A, and L38A, which lie in the N-terminal region and helix II, the Φ_I-values exceed those for Φ_{TS2} ($\Phi_I - \Phi_{TS2} = 0.28$, 0.16, and 0.28, respectively (Table 2)), suggesting that these residues form non-native stabilizing contacts in the intermediate. For 7 of the 10 residues measured, including 2 of the 3 residues for which $\Phi_I > \Phi_{TS2}$, $\Delta\Delta G_{U-N}$ ranges from 3.4 to 11.5 kJ mol^{-1}, confirming the validity of these

Table 2: Folding and Unfolding Kinetics of Im7* in 0.2 M Na_2SO_4, pH 7.0, 10 °C[a]

variant[b]	K_{U-I}[c]	k_{in}	k_{ni}	M_{U-I}[d]	m_{in}	m_{ni}	M_{U-N}[e]	ΔG_{U-I}[f]	ΔG_{U-N}[f]	Φ_I[g,h]	Φ_{TS2}[g,h]
L3A N-term (p.b)	10.4 ± 2.0	420.7 ± 21.3	2.62 ± 0.10	4.65 ± 0.14	0.6 ± 0	−0.45 ± 0	5.70 ± 0.14	−5.5 ± 0.4	−17.5 ± 0.5	0.84 ± 0.32	0.57 ± 0.25
V16A Helix I (b)	7.5 ± 3.4	258.7 ± 34.9	2.79 ± 0.12	4.50± 0.36	0.6 ± 0	−0.53 ± 0	5.63 ± 0.36	−4.8 ± 1.1	−15.4 ± 1.1	0.67 ± 0.18	0.70 ± 0.18
I22V[j] Helix I (b)	39.8 ± 1.1	125.1 ± 1.3	23.64 ± 0.10	4.80 ± 0.00	0.9 ± 0	−0.31 ± 0	5.99 ± 0.00	−8.7 ± 0.1	−12.6 ± 0.1	−0.03 ± 0.10	0.24 ± 0.08
L34A[j] Helix II (p.b)	16.7 ± 0.6	1216.3 ± 96.2	59.22 ± 0.91	4.95 ± 0.08	0.7 ± 0	−0.10 ± 0	5.75 ± 0.08	−6.6 ± 0.1	−13.7 ± 0.2	0.25 ± 0.09	−0.23 ± 0.14
L38A[j] Helix II (p.b)	5.5 ± 2.2	1169.1 ± 0	118.56 ± 24.15	4.40 ± 0.53	0.8 ± 0	−0.11 ± 0.06	5.28 ± 0.54	−4.0 ± 0.9	−9.4 ± 1.1	0.42 ± 0.08	0.13 ± 0.09
V42A Helix II (p.b)	30.0 ± 6.0	459.1 ± 13.7	5.21 ± 0.17	4.43 ± 0.12	0.6 ± 0	−0.53 ± 0	5.56 ± 0.12	−8.0 ± 0.5	−18.5 ± 0.5	0.16 ± 0.34[i]	−0.33 ± 0.56[i]
I44V Helix II (b)	53.2 ± 7.9	113.9 ± 1.6	1.73 ± 0.07	4.85 ± 0.12	0.6 ± 0	−0.30 ± 0	5.75 ± 0.12	−9.3 ± 0.3	−19.2 ± 0.4	−0.16 ± 0.33[i]	0.70 ± 0.56[i]
L53A Helix III (b)	85.7 ± 8.2	80 ± 63.9	165.28 ± 27.12	5.00 ± 0.21	0.6 ± 0	−0.40 ± 0	6.00 ± 0.21	−10.5 ± 0.2	−8.8 ± 1.9	−0.17 ± 0.09	0.07 ± 0.16
I68V Helix IV (b)	8.0 ± 1.0	331.9 ± 12.1	1.74 ± 0.04	4.50 ± 0.10	0.6 ± 0	−0.5 ± 0	5.60 ± 0.10	−4.9 ± 0.3	−17.3 ± 0.3	0.97 ± 0.35	0.86 ± 0.31
V69A Helix IV (b)	26.8 ± 7.4	300.1 ± 12.7	4.42 ± 0.20	4.70 ± 0.20	0.6 ± 0	−0.45 ± 0	5.7 ± 0.20	−7.7 ± 0.6	−17.7 ± 0.7	0.20 ± 0.27	0.15 ± 0.28

[a] Units: [Na_2SO_4] (M), k_{xy} (s^{-1}), m_{xy} (kJ mol^{-1} M^{-1}), ΔG_{X-Y} (kJ mol^{-1}). [b] The location of the residue in the native structure is noted as the corresponding helix, followed by the degree of burial of that side chain in brackets, where p.b. is partially buried, and b. is buried. [c] K_{U-I} is calculated as k_{ui}/k_{iu}. Errors in K_{U-I} are the propagated errors estimated from the partial derivative of that ratio. [d] M_{U-I} calculated from eq 3. [e] M_{U-N} is calculated from eq 4. [f] ΔG_{U-N} and ΔG_{U-I} are estimated from eqs 1 and 2, respectively. [g] Φ_I and Φ_{TS2} are calculated from eqs 9 and 10. [h] Errors in k_{in}, k_{ni} correspond to the fitting errors. m_{ni} was fixed in the fitting procedure, and m_{in} was constrained to the value for the wild-type protein, except for variants showing an unfolding roll-over. Errors in ΔG_{U-N}, ΔG_{U-I}, M_{U-I}, M_{U-N}, Φ_I and Φ_{TS2} are the propagated errors estimated from the partial derivatives of eqs 1, 2, 3, 4, 9 and 10, respectively. [i] Due to the small $\Delta\Delta G_{U-N}$ values obtained for these variants the Φ-value cannot be determined accurately, resulting in high propagated errors. [j] These proteins show roll-over in the unfolding branch in 0.2 M Na_2SO_4 (Figure 5A,C). The kinetic data have been fitted taking the unfolding roll-over into account (see Methods).

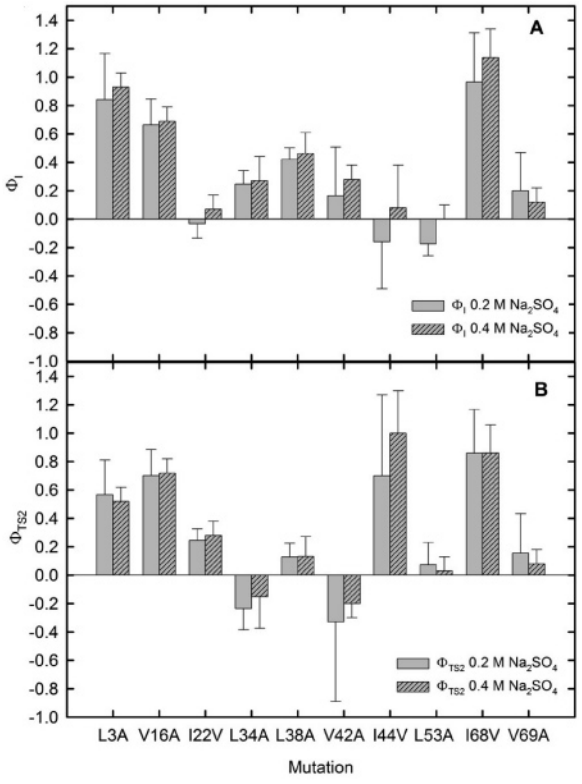

FIGURE 6: Comparison of (A) Φ_I and (B) Φ_{TS2} values obtained in 0.2 M (light gray bars) and 0.4 M (filled gray bars) Na_2SO_4 (*26*) for equivalent variants of Im7*. The error bars were calculated from the fits to the chevron plots as described in the Methods, taking into account the errors in the kinetic constants and slopes resulting from chevron plots. Errors in the data in 0.4 M Na_2SO_4 were taken from previous data (*26*), or were recalculated (see Methods).

conclusions. Statistically, an excellent agreement was obtained for the Φ_I-values obtained in 0.2 and 0.4 M Na_2SO_4 (correlation coefficient of 0.97), as well as for the Φ_{TS2}-values obtained in the two concentrations of Na_2SO_4 employed (correlation coefficient of 0.97), demonstrating that Im7* folds via a three-helical species that is stabilized by both native and non-native interactions, irrespective of the concentration of Na_2SO_4 in which folding is studied.

DISCUSSION

A Single Model Describes the Folding Mechanism of Im7 in Different Concentrations of Na_2SO_4.* Experimental results obtained over the past few years have demonstrated that partially unfolded intermediates are formed during the folding of many proteins, including small proteins with simple topologies such as the bacterial immunity proteins (*41*−*43*). Characterization of these partially folded states and analysis of the folding kinetics using rapid methods have provided detailed information about the role of intermediates in folding, as well as the structural properties of these species (*44*, *45*). In some cases, kinetic information supports an on-pathway role (U ↔ I ↔ N), suggesting that intermediates can be productive, allowing the protein to attain the native structure by consolidation of the packing of side chains from an intermediate species in which the native topology is usually already well formed (*1*, *25*, *46*−*48*). For other proteins, however, intermediates have been suggested to be off-pathway species that are kinetically trapped or substantially misfolded (I ↔ U ↔ N) such that they cannot reach the native state without substantial unfolding and/or reorganization events (*49*−*51*). As shown here and in previous studies (*6*, *47*), the presence of intermediates can be manifested kinetically in many ways, including nonlinearity in the folding branch of the chevron plot, by the presence of an unfolding rollover, or by nonlinearity in both the folding and unfolding branches of the chevron plot. Interpretation of nonlinearity (downward curvature) in the unfolding branch of a chevron plot in terms of the transient population of an intermediate during unfolding is particularly informative, since such a model dictates that the intermediate must be on-pathway, since the same species is populated during both

folding and unfolding (*4*, *37*, *47*). Other scenarios have also been used to rationalize the presence of an unfolding rollover, including a shift between parallel pathways (*52*), proline isomerization processes associated to kinetic coupling of folding (*53*), broad transition-state barriers (*38*), nonideality of denaturant solutions (*10*), aggregation (*10*), or a switch in the rate-determining step (*4*, *22*, *39*). In other cases, rollovers have been fitted using a two-state model including a quadratic term to fit the unfolding curvature (*54*).

In the case of Im7* the presence of a clear rollover in the folding branch of the chevron plot, combined with a very fast folding phase that can be visualized directly by ultrarapid mixing experiments, and monitored indirectly using stopped-flow fluorescence by the presence of a large increase in signal in the burst phase of folding, demonstrates that the folding rollover results from the population of an on-pathway intermediate (*25*, 26). For some variants of Im7*, however, nonlinearity is also observed in the unfolding branch of the chevron plot in 0.2 M and/or 0.4 M Na_2SO_4 (Figure 5 and (*26*)). By studying the effect of changes in the concentration of Na_2SO_4 on the folding landscape of Im7*, including acquisition of accurate experimental data for both the kinetic rate constants and their respective amplitudes, we show here that the folding and unfolding kinetics of Im7* can be described by a model in which folding occurs via the population of an on-pathway intermediate that can be formed transiently during both folding and unfolding, irrespective of the concentration of Na_2SO_4 in the folding and unfolding buffers. Increasing the concentration of Na_2SO_4 also has no effect on the compactness of the intermediate formed during Im7* folding or its structural properties, suggesting that intermediate formation involves a highly specific collapse of the polypeptide chain that is dependent on the amino acid sequence, but is independent of the folding conditions. Most importantly, the data demonstrate the persistence of nonnative stabilizing interactions in the three-helical intermediate, the magnitude of which are independent of the kosmotrope concentration, at least under the conditions analyzed here. This result contrasts with the nonspecific collapse of the polypeptide chain during the folding of the protein S6 in the presence of Na_2SO_4 which results in the formation of an off-pathway and over-compact collapsed state that is generated in the dead-time of folding (*12*). Despite changes in stability of the intermediate, TS2 and native Im7* in the presence of Na_2SO_4, Φ-value analysis shows that the structural features of the intermediate and TS2 are not altered substantially by the concentration of the kosmotrope over the range that could be analyzed (0.2−0.4 M), confirming that the existence of the on-pathway three-helical intermediate during Im7* folding is not induced by the presence of the stabilizing salt. Together with previous results (*5*, *26*), the data demonstrate the robustness of the folding energy landscape of Im7* to perturbation of both the sequence and the refolding conditions, demonstrating that a conformational search via a three-helical intermediate, stabilized by both native and non-native interactions, is an important and generic feature of the folding mechanism of this protein.

ACKNOWLEDGMENT

We thank Thomas Kiefhaber for helpful discussions and Godfrey Beddard for helping with estimation of the Φ-value errors. We thank Claire Friel, Graham Spence, Victoria Morton, Stuart Knowling, and the members of Radford group for their helpful discussions on this work. We thank Keith Ainley for technical assistance and Alison Ashcroft for mass spectrometry.

REFERENCES

1. Roder, H., and Colon, W. (1997) Kinetic role of early intermediates in protein folding. *Curr. Opin. Struct. Biol. 7*, 15−28.
2. Dobson, C. M. (2004) Experimental investigation of protein folding and misfolding. *Methods 34*, 4−14.
3. Bai, Y., Sosnick, T. R., Mayne, L., and Englander, S. W. (1995) Protein folding intermediates: native-state hydrogen exchange. *Science 269*, 192−197.
4. Bachmann, A., and Kiefhaber, T. (2001) Apparent two-state Tendamistat folding is a sequential process along a defined route. *J. Mol. Biol. 306*, 375−386.
5. Gorski, S. A., Capaldi, A. P., Kleanthous, C., and Radford, S. E. (2001) Acidic conditions stabilise intermediates populated during the folding of Im7 and Im9. *J. Mol. Biol. 312*, 849−863.
6. Pradeep, L., and Udgaonkar, J. B. (2002) Differential salt-induced stabilization of structure in the initial folding intermediate ensemble of barstar. *J. Mol. Biol. 324*, 331−347.
7. Teilum, K., Maki, K., Kragelund, B. B., Poulsen, F. M., and Roder, H. (2002) Early kinetic intermediate in the folding of acyl-CoA binding protein detected by fluorescence labeling and ultrarapid mixing. *Proc. Natl Acad. Sci. U.S.A. 99*, 9807−9812.
8. Mayor, U., Grossmann, J. G., Foster, N. W., Freund, S. M., and Fersht, A. R. (2003) The denatured state of engrailed homeodomain under denaturing and native conditions. *J. Mol. Biol. 333*, 977−991.
9. Feng, H., Vu, N. D., and Bai, Y. (2005) Detection of a hidden folding intermediate of the third domain of PDZ. *J. Mol. Biol. 346*, 345−353.
10. Went, H. M., Benitez-Cardoza, C. G., and Jackson, S. E. (2004) Is an intermediate state populated on the folding pathway of ubiquitin? *FEBS Lett. 567*, 333−338.
11. Zhong, S., Rousseau, D. L., and Yeh, S. (2004) Modulation of the folding energy landscape of cytochrome *c* with salt. *J. Am. Chem. Soc. 126*, 13934−13935.
12. Otzen, D. E., and Oliveberg, M. (1999) Salt-induced detour through compact regions of the protein folding landscape. *Proc. Natl. Acad. Sci. U.S.A. 96*, 11746−11751.
13. Ferguson, N., Capaldi, A. P., James, R., Kleanthous, C., and Radford, S. E. (1999) Rapid folding with and without populated intermediates in the homologous four helix proteins Im7 and Im9. *J. Mol. Biol. 286*, 1597−1608.
14. Timasheff, S. N., and Arakawa, T. (1997) Stabilization of protein structure by solvents. in *Protein Structure: a practical approach* (Creighton, T. E., Ed.) 2nd ed., Chapter 14, 349−364, New York, IRL Press.
15. Collins, K. D., and Washabaugh, M. W. (1985) The Hofmeister effect and the behaviour of water at interfaces. *Q. Rev. Biophys. 18*, 323−422.
16. Park, S.-H., O'Neil, K. T., and Roder, H. (1997) An early intermediate in the folding reaction of the B1 domain of protein G contains a nativelike core. *Biochemistry 36*, 14277−14283.
17. Parker, M. J., Dempsey, C. E., Lorch, M., and Clarke, A. R. (1997) Acquisition of native beta-strand topology during the rapid collapse phase of protein folding. *Biochemistry 36*, 13396−13405.
18. Nishimura, C., Uversky, V. N., and Fink, A. L. (2001) Effect of salts on the stability and folding of staphylococcal nuclease. *Biochemistry 40*, 2113-2128.
19. Krantz, B. A., Mayne, L., Rumbley, J., Englander, S. W., and Sosnick, T. R. (2002) Fast and slow intermediate accumulation and the initial barrier mechanism in protein folding. *J. Mol. Biol. 324*, 359−371.
20. Khorasanizadeh, S., Peters, I. D., and Roder, H. (1996) Evidence for a three-state model of protein folding from kinetic analysis of ubiquitin variants with altered core residues. *Nat. Struct. Biol. 3*, 193−205.
21. Kleanthous, C., and Walker, D. (2001) Immunity proteins: enzyme inhibitors that avoid the active site. *Trends Biochem. Sci. 26*, 624−631.
22. Ferguson, N., Li, W., Capaldi, A. P., Kleanthous, C., and Radford, S. E. (2001) Using chimeric immunity proteins to explore the energy landscape for alpha-helical protein folding. *J. Mol. Biol. 307*, 393−405.

23. Friel, C. T., Beddard, G. S., and Radford, S. E. (2004) Switching two-state to three-state kinetics in the helical protein Im9 via the optimisation of stabilising non-native interactions by design. *J. Mol. Biol. 342*, 261−273.
24. Cranz-Mileva, S., Friel, C. T., and Radford, S. E. (2005) Helix stability and hydrophobicity in the folding mechanism of the bacterial immunity protein Im9. *Protein Eng., Des. Sel. 18*, 1−10.
25. Capaldi, A. P., Shastry, M. C. R., Kleanthous, C., Roder H., and Radford, S. E. (2001) Ultra-rapid mixing experiments reveal that the four-helix protein Im7-folds through an on-pathway intermediate. *Nat. Struct. Biol. 1*, 68−72.
26. Capaldi, A. P., Kleanthous, C., and Radford, S. E. (2002) Im7 folding mechanism: misfolding on the path to the native state. *Nat. Struct. Biol. 9*, 209−216.
27. Gorski, S. A., Le Duff, C. S., Capaldi, A. P., Kalverda, A. P., Beddard, G. S., Moore, G. R., and Radford, S. E. (2004) Equilibrium hydrogen exchange reveals extensive hydrogen bonded secondary structure in the on-pathway intermediate of Im7. *J. Mol. Biol. 337*, 183−193.
28. Rodriguez-Mendieta, I. R., Spence, G. R., Gell, C., Radford, S. E., and Smith, D. A. (2005) Ultraviolet resonance Raman studies reveal the environment of tryptophan and tyrosine residues in the native and partially folded States of the E colicin-binding immunity protein Im7. *Biochemistry 44*, 3306−3315.
29. Friel, C. T., Capaldi, A. P., and Radford, S. E. (2003) Structural analysis of the rate-limiting transition states in the folding of Im7 and Im9: similarities and differences in the folding of homologous proteins. *J. Mol. Biol. 326*, 293−305.
30. Sanchez, I. E., and Kiefhaber, T. (2003) Evidence for sequential barriers and obligatory intermediates in apparent two-state protein folding. *J. Mol. Biol. 325*, 367−376.
31. Leffler, J. E. (1953) Parameters for the description of transition states. *Science 117*, 340−341.
32. Itzhaki, L. S., Otzen, D. E., and Fersht, A. R. (1995) The structure of the transition state for folding of chymotrypsin inhibitor 2 analysed by protein engineering methods: evidence for a nucleation-condensation mechanism for protein folding. *J. Mol. Biol. 254*, 260−288.
33. Matouschek, A., Otzen, D. E., Itzhaki, L. S., Jackson, S. E., and Fersht, A. R. (1995) Movement of the position of the transition state in protein folding. *Biochemistry 34*, 13656−13662.
34. Oliveberg, M., Tan, Y. J., Silow, M., and Fersht, A. R. (1998) The changing nature of the protein folding transition state: implications for the shape of the free-energy profile for folding. *J. Mol. Biol. 277*, 933−943.
35. Sanchez, I. E., and Kiefhaber, T. (2003) Hammond behaviour versus ground-state effects in protein folding: evidence for narrow free energy barriers and residual structure in unfolded states. *J. Mol. Biol. 327*, 867−884.
36. Fersht, A. R., and Sato, S. (2004) Phi-value analysis and the nature of protein-folding transition states. *Proc. Natl. Acad. Sci. U.S.A. 101*, 7976−7981.
37. Fersht, A. R. (2000) A kinetically significant intermediate in the folding of barnase. *Proc. Natl. Acad. Sci. U.S.A. 97*, 141221−114126.
38. Otzen, D. E., Kristensen, O., Proctor, M., and Oliveberg, M. (1999) Structural changes in the transition state of protein folding: alternative interpretations of curved chevron plots. *Biochemistry 38*, 6499−6511.
39. Scott, K. A., Randles, L. G., and Clarke, J. (2004) The folding of spectrin domains II: Phi-value analysis of R16. *J. Mol. Biol. 344*, 207−221.
40. Sauder, J. M., MacKenzie, N. E., and Roder, H. (1996) Kinetic mechanism of folding and unfolding of *Rhodobacter capsulatus* cytochrome *c*2. *Biochemistry 35*, 16852−16862.
41. Jackson, S. E. (1998) How do small single-domain proteins fold? *Folding Des. 3*, R81−R91.
42. Baldwin, R. L., and Rose, G. D. (1999) Is protein folding hierarchic? II. Folding intermediates and transition states. *Trends Biochem. Sci. 24*, 77−83.
43. Krantz, B. A., Mayne, L., Rumbley, J., Englander, S. W., and Sosnick, T. R. (2002) Fast and slow intermediate accumulation and the initial barrier mechanism in protein folding. *J. Mol. Biol. 324*, 1−13.
44. Gruebele, M. (1999) The fast protein folding problem. *Annu. Rev. Phys. Chem. 50*, 485−516.
45. Roder, H., Maki, K., Cheng, H., and Shastry, M. C. (2004) Rapid mixing methods for exploring the kinetics of protein folding. *Methods 34*, 15−27.
46. Parker, M. J., and Marqusee, S. (2001) A kinetic folding intermediate probed by native state hydrogen exchange. *J. Mol. Biol. 305*, 593−602.
47. Khan, F., Chuang, J. I., Gianni, S., and Fersht, A. R. (2003) The kinetic pathway of folding of barnase. *J. Mol. Biol. 333*, 169−186.
48. Jemth, P., Gianni, S., Day, R., Li, B., Johnson, C. M., Daggett, V., and Fersht, A. R. (2004) Demonstration of a low-energy on-pathway intermediate in a fast-folding protein by kinetics, protein engineering, and simulation. *Proc. Natl. Acad. Sci. U.S.A. 101*, 6450−6455.
49. Chang, J. Y. (2002) The folding pathway of alpha-lactalbumin elucidated by the technique of disulfide scrambling. Isolation of on-pathway and off-pathway intermediates. *J. Biol. Chem. 277*, 120−126.
50. Kitahara, R., and Akasaka, K. (2003) Close identity of a pressure-stabilized intermediate with a kinetic intermediate in protein folding. *Proc. Natl. Acad. Sci. U.S.A. 100*, 3167−3172.
51. Bollen, Y. J., and van Mierlo, C. P. (2005) Protein topology affects the appearance of intermediates during the folding of proteins with a flavodoxin-like fold. *Biophys. Chem. 114*, 181−189.
52. Dinner, A. R., Sali, A., Smith, L. J., Dobson, C. M., and Karplus, M. (2000) Understanding protein folding via free-energy surfaces from theory and experiment. *Trends Biochem. Sci. 25*, 331−339.
53. Kiefhaber, T., Kohler, H. H., and Schmid, F. X. (1992) Kinetic coupling between protein folding and prolyl isomerization. I. Theoretical models. *J. Mol. Biol. 224*, 217−229.
54. Matouschek, A., Matthews, J. M., Johnson, C. M., and Fersht, A. R. (1994) Extrapolation to water of kinetic and equilibrium data for the unfolding of barnase in urea solutions. *Protein Eng. 7*, 1089−1095.
55. Spence, G. R., Capaldi, A. P., and Radford, S. E. (2004) Trapping the on-pathway folding intermediate of Im7 at equilibrium. *J. Mol. Biol. 341*, 215−226.
56. Sanchez, I. E., and Kiefhaber, T. (2003) Nonlinear rate-equilibrium free energy relationships and Hammond behaviour in protein folding. *Biophys. Chem. 100*, 397−407.

BI0521238